Supporting Information for "Impact of Dynamic Phytoplankton Stoichiometry on Global Scale Patterns of Nutrient Limitation, Nitrogen Fixation, and Carbon Export"

George I. Hagstrom[1], Charles A. Stock[2], Jessica Y. Luo[2], and Simon A.

Levin[1]

[1]Department of Ecology and Evolutionary Biology, Princeton University

[2]NOAA Geophysical Fluid Dynamics Laboratory, Princeton NJ

Contents of this file

Introduction

The Supporting Information contains text sections presenting more detailed mathematical analysis of the dynamic model and its properties, in particular a derivation of the optimal trait values and explanation of how the model incorporates the diel cycle (Text S1), a discussion and figure describing biogeographic patterns of trait investments and their contribution to the P-quota (Text S2 and Figure S1), an analysis of the temperature scaling of rates in the dynamic model and dynamic with translation compensation models

(Text S3 and Figures S2 and S3), a map of biome definitions used to aggregate model predictions over biomes (Figure S4), a map of the differences in N:P between the frugality model and growth rate model (Figure S5), and a table listing all data sources used in this paper for comparisons between model predictions and observations along with the appropriate references (Table S1).

Text S1: Calculating Optimal Strategies

Here we consider the problem of solving for investments in E and L that maximize the growth rate μ. Under our model formulation for photosynthesis rates, the photosynthetic functional response depends linearly on the total investment $L = F_1 + F_2$, with a more complex dependence on the individual F_1 and F_2 investments. To see this let $F_2 = cL$, with $F_1 = (1 - c)L$. Then, if we let $P_s = \min\left(k_1(1 - c), k_2 c\right)$, we find after substituting in Main text Eq. 19:

$$\mu_{\text{light}} = \frac{LP_s \left(1 - \exp\left(-\frac{\alpha\theta cIrr}{P_s}\right)\right) - bresp}{1 + \zeta} \tag{1}$$

Note how μ_{light} depends linearly on L for fixed choice of c, because L does not appear inside the exponential. For a given irradiance Irr, we can find the growth maximizing solution by first solving for the value of c that maximizes the coefficient of L in the above expression:

$$P_{\text{spec}} = \max_{c \in [0,1]} P_s \left(1 - \exp\left(-\frac{\alpha\theta cIrr}{P_s}\right)\right) \tag{2}$$

We define the function $c^*(Irr)$ as the value of c that maximizes this expression. Using this $c^*(Irr)$, which we can efficiently compute offline, we can find optimal solutions in constant light environments. However, the dynamic ATOM-COBALT model resolves irradiance over the diel cycle, and fully accounting for this in computing optimal allocations

would dramatically increase the computational complexity and make this model unsuitable for use in global-scale simulations. Instead, we will model phytoplankton resource allocations by assuming phytoplankton maximize growth in an environment with constant irradiance over the light period, and zero irradiance over the dark period. Phytoplankton will retain memory of the mean irradiance during the day and the length of the day.

We will calculate optimal strategies under the assumption that light is constant over the day, which has length fraction D and irradiance Irr_{day}. In each grid cell, ATOM-COBALT computes the day-time irradiance and the day-length using an exponential memory term, and we assume that phytoplankton living in that grid cell have access to these estimates. Under the assumption of constant irradiance during the day, and 0 irradiance during the night, the photosynthesis limitation term becomes:

$$\mu_{\text{light}} = \frac{DLP_{\text{spec}}(Irr_{\text{day}}) - bresp}{1 + \zeta} \tag{3}$$

There exist two scenarios for optimal strategies: they can occur either on the line $E^* + L^* + S = 1$, or beneath it: $E^* + L^* + S < 1$.

First we consider the scenario in which all three growth rates are equal. Here $E^* = $ nutlim, and we can solve for L^*:

$$L^* = \frac{P_{\text{cmax}}E^*\left(1 + \zeta\right) + bresp}{DP_{\text{spec}}(Irr_{\text{day}})} \tag{4}$$

This solution (E^*, L^*) is only valid if $E^* + L^* + S \leq 1$. If the solution is invalid, it means that nutrient concentrations are so high that the optimal strategy would fill more space than the cell has available. If this happens, the optimal strategy will instead be a maximum growth rate strategy, balancing synthesis and light limitation under the constraint that $E^* + L^* + S = 1$, which leads to the following equation:

:

$$E^* + \frac{P_{\mathrm{cmax}}E^*(1+\zeta) + bresp}{DP_{\mathrm{spec}}(Irr_{\mathrm{day}})} + S - 1 = 0 \tag{5}$$

This equation is linear and has exact solution:

$$E^* = \frac{(1-S)\,DP_{\mathrm{spec}}(Irr_{\mathrm{day}}) - bresp}{DP_{\mathrm{spec}}(Irr_{\mathrm{day}}) + P_{\mathrm{cmax}}(1+\zeta)} \tag{6}$$

We modify the optimal solution arising from these heuristics by multiplying the total allocation to light harvesting by a constant factor L_{fac}, so that:

$$E^{\mathrm{opt}} = \mathrm{nutlim} \tag{7}$$

$$L^{\mathrm{opt}} = \left(\frac{P_{\mathrm{cmax}}E^{\mathrm{opt}}(1+\zeta) + bresp}{DP_{\mathrm{spec}}(Irr_{\mathrm{day}})}\right) L_{fac} \tag{8}$$

if $E_{\mathrm{opt}} + L_{\mathrm{opt}} + S \leq 1$, and

$$E^{\mathrm{opt}} = \frac{(1-S)\,DP_{\mathrm{spec}}(Irr_{\mathrm{day}}) - L_{fac}bresp}{DP_{\mathrm{spec}}(Irr_{\mathrm{day}}) + P_{\mathrm{cmax}}(1+\zeta)\,L_{fac}} \tag{9}$$

$$L^{\mathrm{opt}} = \left(\frac{P_{\mathrm{cmax}}E^{\mathrm{opt}}(1+\zeta) + bresp}{DP_{\mathrm{spec}}(Irr_{\mathrm{day}})}\right) L_{fac} \tag{10}$$

otherwise.

This factor accounts for the fact that the heuristic solution will not be the optimal solution in a real light environment, but that it might systematically over or underestimate the optimal constant allocation to light harvesting relative to biosynthesis. We determine L_{fac} using simulations, comparing the levels of light limitation to synthesis limitation and setting the factor so that the two are as close as possible over a range of different light levels.

To determine actual phytoplankton growth rates in dynamic light environments, we assume that phytoplankton perform nutrient uptake and biosynthesis throughout the entire diel period, but can only acquire carbon at a rate governed by the instantaneous irradiance. We model the decoupling between carbon acquisition and nutrient uptake/synthesis

by introducing an irradiance memory, which measures the average growth rate implied by carbon acquisition over the previous day (using an exponential forgetting). Then the instantaneous growth rate realized by the cell is the minimum of the growth rate from irradiance memory and from synthesis limitation:

$$\mu = \min\left(P_{\mathrm{cmax}}E^{opt}, \int_{-\infty}^{t} dt' \left(\frac{L^{\mathrm{opt}}P_{\mathrm{spec}}\left(1 - \exp\left(-\frac{\alpha\theta c Irr_{\mathrm{inst}}}{P_{\mathrm{spec}}}\right)\right) - bresp}{1 + \zeta}\right) \frac{\exp\left(-(t - t')/t_{day}\right)}{t_{day}}\right),$$
(11)

where t_{day} is the length of a day.

Text S2: Global Distribution of Optimal Strategies

To show how phytoplankton N:P emerges in ATOM-COBALT, we computed and plotted the contribution of each modeled phosphorus pool to cell phosphorus quotas (Fig. S1). Average values were computed over the entire euphotic zone, weighting by the depth profile of small and large phytoplankton biomass and the level of total export from the euphotic zone. The contribution of biosynthesis investments to the P-quota peaks in productive ecosystems and declines towards oligotrophic gyres, with an opposite trend in the contribution of the structural pool. Although luxury P-storage also declines from HNLC regions towards gyres, its contribution exhibits a different pattern than that of biosynthesis, being relatively elevated in tropical regions and the Pacific ocean while being depressed in the Atlantic.

Text S3: Temperature Dependence of Growth Rates

Main text Eq. 19 describes the photosynthetic functional response in ATOM-COBALT (including the dynamic model and all alternative models), repeated here:

$$\mu_{\mathrm{light}} = \frac{P_{\mathrm{m}}\left(1 - \exp\left(-\frac{\alpha\phi_M \mathrm{F_2Irr}}{P_{\mathrm{m}}}\right)\right) - bresp}{1 + \zeta}.$$

October 2, 2023, 4:24pm

Temperature enters this equation in two places: P_m is proportional to $\exp\left(\kappa_{\mathrm{photo}}T\right)$ and $bresp$ is proportional to $\exp\left(\kappa_{\mathrm{eppley}}T\right)$. However, the temperature scaling of the first term on the right hand side depends on the value of irradiance. When $Irr \ll \frac{P_{\mathrm{m}}}{\alpha\phi_M \mathrm{F}_2}$, we can perform a Taylor expansion in powers of Irr and dropping terms higher than first order we find that (and for now assuming that investments are fixed and not being optimized):

$$\mu_{\mathrm{light}} = \frac{(\alpha\phi_M \mathrm{F}_2 Irr) - bresp}{1 + \zeta}$$

All terms containing P_m canceled from this expression, and it does not depend on the value of κ_{photo}. The only temperature dependence in this expression comes through b_{resp}, which is an exponentially increasing cost.

In the other limit, $Irr \gg \frac{P_{\mathrm{m}}}{\alpha\phi_M \mathrm{F}_2}$, the exponential term can be dropped and:

$$\mu_{\mathrm{light}} = \frac{P_m - b_{\mathrm{resp}}}{1 + \zeta}$$

This expression also depends on temperature through the term P_m. These results suggest that when Irr is small, photosynthetic carbon fixation doesn't scale with temperature, and when Irr is large, it scales exponentially with coefficient κ_{photo}. Fig S2 shows how this effect manifests for the dynamic model ($\kappa_{\mathrm{photo}} = \kappa_{\mathrm{eppley}}$) and for the dynamic with translation-compensation model ($\kappa_{\mathrm{photo}} = 0$). In both cases, the realized growth dependence on temperature scales more slowly than κ_{eppley}, however in the dynamic with translation compensation model this is universal across all irradiance levels whereas in dynamic the temperature dependence at high irradiance is close to κ_{eppley}. This change drives differences between the two models in high-temperature, high irradiance environments.

Fig. S3 show the impact of temperature on N:P for small phytoplankton in the dynamic and the dynamic with translation compensation model over the same range of irradiance values. The response of N:P ratios reflects the temperature response, growth rate having a weak temperature scaling is accompanied by a large increase in N:P with temperature. In the dynamic with translation compensation model this effect occurs at all levels of irradiance, but the figure also shows a weaker increase in N:P with temperature at low irradiance in the ATOM-COBALT simulations.

References

Adcroft, A., Anderson, W., Balaji, V., Blanton, C., Bushuk, M., Dufour, C. O., . . . others (2019). The GFDL global ocean and sea ice model OM4. 0: Model description and simulation features. *Journal of Advances in Modeling Earth Systems*, *11*(10), 3167–3211.

Baer, S. E., Lomas, M. W., Terpis, K. X., Mouginot, C., & Martiny, A. C. (2017). Stoichiometry of Prochlorococcus, Synechococcus, and small eukaryotic populations in the western North Atlantic Ocean. *Environmental microbiology*, *19*(4), 1568–1583.

Baker, A. R., & Croot, P. L. (2010). Atmospheric and marine controls on aerosol iron solubility in seawater. *Marine Chemistry*, *120*(1-4), 4–13.

Behrenfeld, M. J., Boss, E., Siegel, D. A., & Shea, D. M. (2005). Carbon-based ocean productivity and phytoplankton physiology from space. *Global biogeochemical cycles*, *19*(1).

Bode, A., Varela, M. M., Teira, E., Fernández, E., González, N., & Varela, M. (2004). Planktonic carbon and nitrogen cycling off northwest Spain: variations in production

of particulate and dissolved organic pools. *Aquatic Microbial Ecology*, *37*(1), 95–107.

Bopp, L., Aumont, O., Kwiatkowski, L., Clerc, C., Dupont, L., Ethé, C., ... Tagliabue, A. (2022). Diazotrophy as a key driver of the response of marine net primary productivity to climate change. *Biogeosciences*, *19*(17), 4267–4285.

Bopp, L., Resplandy, L., Orr, J. C., Doney, S. C., Dunne, J. P., Gehlen, M., ... Seferian, R. (2013). Multiple stressors of ocean ecosystems in the 21st century: projections with CMIP5 models. *Biogeosciences*, *10*, 6225–6245.

Capone, D. G., Zehr, J. P., Paerl, H. W., Bergman, B., & Carpenter, E. J. (1997). Trichodesmium, a globally significant marine cyanobacterium. *Science*, *276*(5316), 1221–1229.

Charpy, L., Dufour, P., & Garcia, N. (1997). Particulate organic matter in sixteen Tuamotu atoll lagoons (French Polynesia). *Marine Ecology Progress Series*, *151*, 55–65.

Chien, C.-T., Pahlow, M., Schartau, M., Li, N., & Oschlies, A. (2023). Effects of phytoplankton physiology on global ocean biogeochemistry and climate. *Science Advances*, *9*(30), eadg1725.

Clemente, T. M., Ernst, J., Fong, A., Updyke, B., Viviani, D., Weersing, K., ... Karl, D. (2010). SUPER HI-CAT: Survey of Underwater Plastic and Ecosystem Response between Hawaii and California. In *Proceedings from the 2010 AGU Ocean Sciences Meeting*.

Copin-Montegut, C., & Copin-Montegut, G. (1978). The chemistry of particulate matter from the south Indian and Antarctic oceans. *Deep Sea Research*, *25*(10), 911–931.

Copin-Montegut, C., & Copin-Montegut, G. (1983). Stoichiometry of carbon, nitrogen,

and phosphorus in marine particulate matter. *Deep Sea Research Part A. Oceanographic Research Papers*, *30*(1), 31–46.

Daines, S. J., Clark, J. R., & Lenton, T. M. (2014). Multiple environmental controls on phytoplankton growth strategies determine adaptive responses of the N:P ratio. *Ecology letters*, *17*(4), 414–425.

Danabasoglu, G., Lamarque, J.-F., Bacmeister, J., Bailey, D., DuVivier, A., Edwards, J., ... others (2020). The community earth system model version 2 (CESM2). *Journal of Advances in Modeling Earth Systems*, *12*(2), e2019MS001916.

Deutsch, C., & Weber, T. (2012). Nutrient ratios as a tracer and driver of ocean biogeochemistry. *Annual Review of Marine Science*, *4*(1), 113–141.

Devault, D. (1980). Quantum mechanical tunnelling in biological systems. *Quarterly reviews of biophysics*, *13*(4), 387–564.

DeVries, T., & Deutsch, C. (2014). Large-scale variations in the stoichiometry of marine organic matter respiration. *Nature Geoscience*, *7*(12), 890–894.

Dietze, H., Oschlies, A., & Kähler, P. (2004). Internal-wave-induced and double-diffusive nutrient fluxes to the nutrient-consuming surface layer in the oligotrophic subtropical North Atlantic. *Ocean Dynamics*, *54*, 1–7.

Dunne, J., Horowitz, L., Adcroft, A., Ginoux, P., Held, I., John, J., ... others (2020). The GFDL Earth System Model version 4.1 (GFDL-ESM 4.1): Overall coupled model description and simulation characteristics. *Journal of Advances in Modeling Earth Systems*, *12*(11), e2019MS002015.

Dunne, J. P., John, J. G., Shevliakova, E., Stouffer, R. J., Krasting, J. P., Malyshev, S. L., ... others (2013). GFDL's ESM2 global coupled climate–carbon earth system

models. Part II: carbon system formulation and baseline simulation characteristics. *Journal of Climate*, *26*(7), 2247–2267.

Dunne, J. P., Sarmiento, J. L., & Gnanadesikan, A. (2007). A synthesis of global particle export from the surface ocean and cycling through the ocean interior and on the seafloor. *Global Biogeochemical Cycles*, *21*(4).

Elser, J., Sterner, R. W., Gorokhova, E., Fagan, W., Markow, T., Cotner, J. B., ... Weider, L. (2000). Biological stoichiometry from genes to ecosystems. *Ecology Letters*, *3*(6), 540–550.

Emerson, S. (2014). Annual net community production and the biological carbon flux in the ocean. *Global Biogeochemical Cycles*, *28*(1), 14–28.

Eppley, R. W. (1972). Temperature and phytoplankton growth in the sea. *Fish. Bull.*, *70*(4), 1063–1085.

Fichaut, M., Garcia, M., Giorgetti, A., Iona, A., Kuznetsov, A., Rixen, M., & Group, M. (2003). MEDAR/MEDATLAS 2002: A Mediterranean and Black Sea database for operational oceanography. In *Elsevier oceanography series* (Vol. 69, pp. 645–648). Elsevier.

Galbraith, E. D., & Martiny, A. C. (2015). A simple nutrient-dependence mechanism for predicting the stoichiometry of marine ecosystems. *Proceedings of the National Academy of Sciences*, *112*(27), 8199–8204.

Garcia, C. A., Baer, S. E., Garcia, N. S., Rauschenberg, S., Twining, B. S., Lomas, M. W., & Martiny, A. C. (2018). Nutrient supply controls particulate elemental concentrations and ratios in the low latitude eastern Indian Ocean. *Nature communications*, *9*(1), 4868.

Garcia, C. A., Hagstrom, G. I., Larkin, A. A., Ustick, L. J., Levin, S. A., Lomas, M. W., & Martiny, A. C. (2020). Linking regional shifts in microbial genome adaptation with surface ocean biogeochemistry. *Philosophical Transactions of the Royal Society B*, *375*(1798), 20190254.

Garcia, H., Locarnini, R., Boyer, T., Antonov, J., Baranova, O., Zweng, M., ... Johnson, D. (2014). World Ocean Atlas 2013, Volume 4: Dissolved Inorganic Nutrients (Phosphate, Nitrate, Silicate), NOAA Atlas NESDIS, vol. 76, edited by S. Levitus, 25 pp. *US Gov. Print. Off., Washington, DC*.

Garcia, H. E., Locarnini, R. A., Boyer, T. P., Antonov, J. I., Baranova, O. K., Zweng, M. M., ... Levitus, S. (2013). *World Ocean Atlas 2013: Dissolved Inorganic Nutrients (phosphate, Nitrate, Silicate)*. US Department of Commerce, National Oceanic and Atmospheric Administration.

Garcia, N. S., Talmy, D., Fu, W.-W., Larkin, A. A., Lee, J., & Martiny, A. C. (2022). The diel cycle of surface ocean elemental stoichiometry has implications for ocean productivity. *Global Biogeochemical Cycles*, *36*(3), e2021GB007092.

Gasol, J. M., Vázquez-Domínguez, E., Vaqué, D., Agustí, S., & Duarte, C. M. (2009). Bacterial activity and diffusive nutrient supply in the oligotrophic Central Atlantic Ocean. *Aquatic Microbial Ecology*, *56*(1), 1–12.

Geider, R., MacIntyre, H., & Kana, T. (1997). Dynamic model of phytoplankton growth and acclimation: responses of the balanced growth rate and the chlorophyll a: carbon ratio to light, nutrient-limitation and temperature. *Marine Ecology Progress Series*, *148*, 187–200.

Großkopf, T., Mohr, W., Baustian, T., Schunck, H., Gill, D., Kuypers, M. M., ...

LaRoche, J. (2012). Doubling of marine dinitrogen-fixation rates based on direct measurements. *Nature*, *488*(7411), 361–364.

Hagstrom, G., Stock, C., Luo, J., & Levin, S. (2023, September). *Simulation data for "Impact of Dynamic Phytoplankton Stoichiometry on Global Scale Patterns of Nutrient Limitation, Nitrogen Fixation, and Carbon Export".* Zenodo. Retrieved from `https://doi.org/10.5281/zenodo.8393830` doi: 10.5281/zenodo.8393830

Hagstrom, G. I., & Levin, S. A. (2017). Marine Ecosystems as Complex Adaptive Systems: Emergent Patterns, Critical Transitions, and Public Goods. *Ecosystems*, *20*(3), 458–476. Retrieved from `https://link.springer.com/article/10.1007/s10021-017-0114-3`

Hewson, I., Paerl, R. W., Tripp, H. J., Zehr, J. P., & Karl, D. M. (2009). Metagenomic potential of microbial assemblages in the surface waters of the central Pacific Ocean tracks variability in oceanic habitat. *Limnology and Oceanography*, *54*(6), 1981–1994.

Horowitz, L. W., Walters, S., Mauzerall, D. L., Emmons, L. K., Rasch, P. J., Granier, C., . . . others (2003). A global simulation of tropospheric ozone and related tracers: Description and evaluation of MOZART, version 2. *Journal of Geophysical Research: Atmospheres*, *108*(D24).

Inomura, K., Deutsch, C., Jahn, O., Dutkiewicz, S., & Follows, M. J. (2022). Global patterns in marine organic matter stoichiometry driven by phytoplankton ecophysiology. *Nature Geoscience*, *15*(12), 1034–1040.

Karl, D. M., Björkman, K. M., Dore, J. E., Fujieki, L., Hebel, D. V., Houlihan, T., . . . Tupas, L. M. (2001). Ecological nitrogen-to-phosphorus stoichiometry at station

ALOHA. *Deep Sea Research Part II: Topical Studies in Oceanography*, *48*(8-9), 1529–1566.

Klausmeier, C. A., Litchman, E., Daufresne, T., & Levin, S. A. (2004). Optimal nitrogen-to-phosphorus stoichiometry of phytoplankton. *Nature*, *429*(6988), 171.

Kulk, G., Platt, T., Dingle, J., Jackson, T., Jönsson, B. F., Bouman, H. A., . . . others (2020). Primary production, an index of climate change in the ocean: satellite-based estimates over two decades. *Remote Sensing*, *12*(5), 826.

Kwiatkowski, L., Aumont, O., Bopp, L., & Ciais, P. (2018). The impact of variable phytoplankton stoichiometry on projections of primary production, food quality, and carbon uptake in the global ocean. *Global Biogeochemical Cycles*, *32*(4), 516–528.

Kwiatkowski, L., Torres, O., Bopp, L., Aumont, O., Chamberlain, M., Christian, J. R., . . . others (2020). Twenty-first century ocean warming, acidification, deoxygenation, and upper-ocean nutrient and primary production decline from CMIP6 model projections. *Biogeosciences*, *17*(13), 3439–3470.

Kwon, E. Y., Sreeush, M., Timmermann, A., Karl, D. M., Church, M. J., Lee, S.-S., & Yamaguchi, R. (2022). Nutrient uptake plasticity in phytoplankton sustains future ocean net primary production. *Science Advances*, *8*(51), eadd2475.

Large, W., & Yeager, S. (2009). The global climatology of an interannually varying air–sea flux data set. *Climate dynamics*, *33*(2), 341–364.

Larkin, A., Lee, J. A., & Martiny, A. C. (2020). *POC, PON, and POP from surface underway water samples collected during AMT28/JR18001.* (Tech. Rep.). British Oceanographic Data Centre, National Oceanography Centre, NERC, UK. (https://doi.org/10.5285/d76d90bb-5d7a-5415-e053- 6c86abc0d182)

Lauvset, S. K., Key, R. M., Olsen, A., Van Heuven, S., Velo, A., Lin, X., ... others (2016). A new global interior ocean mapped climatology: The 1× 1 GLODAP version 2. *Earth System Science Data*, *8*(2), 325–340.

Lee, J. A., Garcia, C. A., Larkin, A. A., Carter, B. R., & Martiny, A. C. (2021). Linking a latitudinal gradient in ocean hydrography and elemental stoichiometry in the eastern Pacific Ocean. *Global Biogeochemical Cycles*, *35*(5), e2020GB006622.

Lenton, T. M., & Watson, A. J. (2000). Redfield revisited: 1. Regulation of nitrate, phosphate, and oxygen in the ocean. *Global biogeochemical cycles*, *14*(1), 225–248.

Litchman, E., & Klausmeier, C. A. (2008). Trait-based community ecology of phytoplankton. *Annual Review of Ecology, Evolution, and Systematics*, *39*, 615–639.

Loh, A. N., & Bauer, J. E. (2000). Distribution, partitioning and fluxes of dissolved and particulate organic C, N and P in the eastern North Pacific and Southern Oceans. *Deep Sea Research Part I: Oceanographic Research Papers*, *47*(12), 2287–2316.

Lomas, M. W., Baer, S. E., Mouginot, C., Terpis, K. X., Lomas, D. A., Altabet, M. A., & Martiny, A. C. (2021). Varying influence of phytoplankton biodiversity and stoichiometric plasticity on bulk particulate stoichiometry across ocean basins. *Communications Earth & Environment*, *2*(1), 143.

Lomas, M. W., Burke, A., Lomas, D., Bell, D., Shen, C., Dyhrman, S. T., & Ammerman, J. W. (2010). Sargasso Sea phosphorus biogeochemistry: an important role for dissolved organic phosphorus (DOP). *Biogeosciences*, *7*(2), 695–710.

Lomas, M. W., & Martiny, A. C. (2020a). *Depth profile data from R/V Atlantic explorer AE1319 in the NW Atlantic from Aug-Sept. 2013 (Version 1) [Data set]* (Tech. Rep.). Biological and Chemical Oceanography Data Management Office (BCO-

DMO). (https://doi.org/10.26008/1912/BCO-DMO.829797.1)

Lomas, M. W., & Martiny, A. C. (2020b). *Depth profle data from Bermuda Atlantic Time-Series Validation cruise 46 (BVAL46) in the Sargasso Sea from Sept-Oct. 2011* (Tech. Rep.). Biological and Chemical Oceanography Data Management Office (BCO-DMO). (https://doi. org/10.26008/1912/bco-dmo.829843.1)

Lomas, M. W., & Martiny, A. C. (2020c). *Depth profle data from R/V New Horizons NH1418 in the tropical Pacifc from Sept-Oct 2014* (Tech. Rep.). Biological and Chemical Oceanography Data Management Office (BCO-DMO). (https://doi.org/10.26008/1912/bco-dmo.829895.1)

Long, M. C., Moore, J. K., Lindsay, K., Levy, M., Doney, S. C., Luo, J. Y., . . . Sylvester, Z. T. (2021). Simulations with the marine biogeochemistry library (MARBL). *Journal of Advances in Modeling Earth Systems*, *13*(12), e2021MS002647.

Luo, Y.-W., Doney, S., Anderson, L., Benavides, M., Berman-Frank, I., Bode, A., . . . others (2012). Database of diazotrophs in global ocean: abundance, biomass and nitrogen fixation rates. *Earth System Science Data*, *4*(1), 47–73.

Martiny, A. C., Garcia, C. A., Lee, J. A., Moreno, A. R., & Larkin, A. A. (2020). *POM concentrations for carbon, nitrogen, phosphorus, and chemical oxygen from GO-SHIP Line P18 Legs 1 and 2 in 2016 and 2017* (Tech. Rep.). Biological and Chemical Oceanography Data Management Office (BCO-DMO). (https://doi.org/10.26008/1912/bco-dmo.816347.1)

Martiny, A. C., Garcia, C. A., Moreno, A. R., & Tanioka, T. (2022). *POM concentrations for carbon, nitrogen, and phosphorus from GO-SHIP Line I07N RB1803 in the Western Indian Ocean from April to June 2018 (Ocean Stoichiometry Project)* (Tech.

Rep.). Biological and Chemical Oceanography Data Management Office (BCO-DMO). (https://doi.org/10.26008/1912/bco-dmo.879076.1 (2022))

Martiny, A. C., Hagstrom, G. I., DeVries, T., Letscher, R. T., Britten, G. L., Garcia, C. A., ... others (2022). Marine phytoplankton resilience may moderate oligotrophic ecosystem responses and biogeochemical feedbacks to climate change. *Limnology and Oceanography*, *67*, S378–S389.

Martiny, A. C., & Lomas, M. W. (2021). *Particulate organic matter (PON, POC, POP) concentrations collected on R/V Roger Revelle cruise RR1604 along the hydrographic line IO9 in the Eastern Indian Ocean from March to April 2016* (Tech. Rep.). Biological and Chemical Oceanography Data Management Office (BCO-DMO). (https://doi.org/10.26008/1912/bco-dmo.734915.3)

Martiny, A. C., Lomas, M. W., Fu, W., Boyd, P. W., Chen, Y.-l. L., Cutter, G. A., ... others (2019). Biogeochemical controls of surface ocean phosphate. *Science advances*, *5*(8), eaax0341.

Martiny, A. C., Pham, C. T., Primeau, F. W., Vrugt, J. A., Moore, J. K., Levin, S. A., & Lomas, M. W. (2013). Strong latitudinal patterns in the elemental ratios of marine plankton and organic matter. *Nature Geoscience*, *6*(4), 279.

Martiny, A. C., Vrugt, J. A., & Lomas, M. W. (2014). Concentrations and ratios of particulate organic carbon, nitrogen, and phosphorus in the global ocean. *Scientific Data*, *1*, 140048.

Martiny, A. C., Vrugt, J. A., Primeau, F. W., & Lomas, M. W. (2013). Regional variation in the particulate organic carbon to nitrogen ratio in the surface ocean. *Global Biogeochemical Cycles*, *27*(3), 723–731.

Matsumoto, K., Tanioka, T., & Rickaby, R. (2020). Linkages between dynamic phytoplankton c: N: P and the ocean carbon cycle under climate change. *Oceanography*, *33*(2), 44–52.

Moore, J. K., Fu, W., Primeau, F., Britten, G. L., Lindsay, K., Long, M., ... Randerson, J. T. (2018). Sustained climate warming drives declining marine biological productivity. *Science*, *359*(6380), 1139–1143.

Moreno, A. R., Garcia, C. A., Larkin, A. A., Lee, J. A. A., Wang, W.-L., Moore, J. K., ... Martiny, A. C. (2020). Latitudinal gradient in the respiration quotient and the implications for ocean oxygen availability. *Proceedings of the National Academy of Sciences*, *117*(37), 22866–22872.

Moreno, A. R., Hagstrom, G. I., Primeau, F. W., Levin, S. A., & Martiny, A. C. (2018). Marine phytoplankton stoichiometry mediates nonlinear interactions between nutrient supply, temperature, and atmospheric CO2. *Biogeosciences*, *15*(9), 2761–2779.

Moreno, A. R., Larkin, A. A., Lee, J. A., Gerace, S. D., Tarran, G. A., & Martiny, A. C. (2022). Regulation of the respiration quotient across ocean basins. *AGU Advances*, *3*(5), e2022AV000679.

Moreno, A. R., & Martiny, A. C. (2018). Ecological stoichiometry of ocean plankton. *Annual review of marine science*, *10*, 43–69.

Moutin, T., Karl, D. M., Duhamel, S., Rimmelin, P., Raimbault, P., Van Mooy, B. A., & Claustre, H. (2008). Phosphate availability and the ultimate control of new nitrogen input by nitrogen fixation in the tropical Pacific Ocean. *Biogeosciences*, *5*(1), 95–109.

O'Neill, R., DeAngelis, D., Pastor, J., Jackson, B., & Post, W. (1989). Multiple nutrient

limitations in ecological models. *Ecological Modelling*, *46*(3-4), 147–163.

O'neill, R., DeAngelis, D., Pastor, J., Jackson, B., & Post, W. (1989). Multiple nutrient
limitations in ecological models. *Ecological Modelling*, *46*(3-4), 147–163.

Pahlow, M., Chien, C.-T., Arteaga, L. A., & Oschlies, A. (2020). Optimality-based non-
redfield plankton–ecosystem model (opem v1. 1) in uvic-escm 2.9–part 1: Implemen-
tation and model behaviour. *Geoscientific Model Development*, *13*(10), 4663–4690.

Passow, U., & Peinert, R. (1993). The role of plankton in particle flux: Two case
studies from the northeast Atlantic. *Deep Sea Research Part II: Topical Studies in
Oceanography*, *40*(1-2), 573–585.

Penn, J. L., & Deutsch, C. (2022). Avoiding ocean mass extinction from climate warming.
Science, *376*(6592), 524–526.

Polovina, J. J., Dunne, J. P., Woodworth, P. A., & Howell, E. A. (2011). Projected
expansion of the subtropical biome and contraction of the temperate and equatorial
upwelling biomes in the north pacific under global warming. *ICES Journal of Marine
Science*, *68*(6), 986–995.

Purcell, E. M. (1977). Life at low Reynolds number. *American Journal of Physics*,
45(1), 3–11.

Rabalais, N. N., Turner, R. E., & Wiseman Jr, W. J. (2002). Gulf of Mexico hypoxia,
aka "The dead zone". *Annual Review of ecology and Systematics*, *33*(1), 235–263.

Raven, J. A., & Geider, R. J. (1988). Temperature and algal growth. *New phytologist*,
110(4), 441–461.

Redfield, A. C. (1958). The biological control of chemical factors in the environment.
American Scientist, *46*(3), 230A–221.

Rhee, G.-Y. (1974). Phosphate uptake under nitrate limitation by scenedesmus sp. and its ecological implications 1. *Journal of Phycology*, *10*(4), 470–475.

Rodier, M., & Le Borgne, R. (1997). Export flux of particles at the equator in the Western and Central Pacific Ocean. *Deep Sea Research Part II: Topical Studies in Oceanography*, *44*(9-10), 2085–2113.

Sarmiento, J. L., & Gruber, N. (2006). *Ocean biogeochemical dynamics*. Princeton University Press.

Séférian, R., Berthet, S., Yool, A., Palmieri, J., Bopp, L., Tagliabue, A., ... others (2020). Tracking improvement in simulated marine biogeochemistry between CMIP5 and CMIP6. *Current Climate Change Reports*, *6*(3), 95–119.

Seitzinger, S. P., Harrison, J. A., Dumont, E., Beusen, A. H., & Bouwman, A. (2005). Sources and delivery of carbon, nitrogen, and phosphorus to the coastal zone: An overview of Global Nutrient Export from Watersheds (NEWS) models and their application. *Global Biogeochemical Cycles*, *19*(4).

Shuter, B. (1979). A model of physiological adaptation in unicellular algae. *Journal of theoretical biology*, *78*(4), 519–552.

Smith, S. L., Pahlow, M., Merico, A., & Wirtz, K. W. (2011). Optimality-based modeling of planktonic organisms. *Limnology and Oceanography*, *56*(6), 2080–2094.

Sterner, R. W., & Elser, J. J. (2017). Ecological Stoichiometry. In *Ecological stoichiometry.* Princeton University Press.

Stock, C. A., Dunne, J. P., Fan, S., Ginoux, P., John, J., Krasting, J. P., ... Zadeh, N. (2020). Ocean biogeochemistry in GFDL's Earth System Model 4.1 and its response to increasing atmospheric CO2. *Journal of Advances in Modeling Earth Systems*,

12(10), e2019MS002043.

Stock, C. A., Dunne, J. P., & John, J. G. (2014). Global-scale carbon and energy flows through the marine planktonic food web: An analysis with a coupled physical–biological model. *Progress in Oceanography*, *120*, 1–28.

Tagliabue, A., Kwiatkowski, L., Bopp, L., Butenschön, M., Cheung, W., Lengaigne, M., & Vialard, J. (2021). Persistent uncertainties in ocean net primary production climate change projections at regional scales raise challenges for assessing impacts on ecosystem services. *Frontiers in Climate*, 149.

Talmy, D., Blackford, J., Hardman-Mountford, N. J., Dumbrell, A. J., & Geider, R. J. (2013). An optimality model of photoadaptation in contrasting aquatic light regimes. *Limnology and Oceanography*, *58*(5), 1802–1818.

Tang, W., Wang, S., Fonseca-Batista, D., Dehairs, F., Gifford, S., Gonzalez, A. G., . . . Cassar, N. (2019). Revisiting the distribution of oceanic N2 fixation and estimating diazotrophic contribution to marine production. *Nature Communications*, *10*(1), 1–10.

Tanioka, T., Garcia, C. A., Larkin, A. A., Garcia, N. S., Fagan, A. J., & Martiny, A. C. (2022). Global patterns and predictors of C:N:P in marine ecosystems. *Communications Earth & Environment*, *3*(1), 271.

Tanioka, T., Larkin, A. A., Moreno, A. R., Brock, M. L., Fagan, A. J., Garcia, C. A., . . . others (2022). Global Ocean Particulate Organic Phosphorus, Carbon, Oxygen for Respiration, and Nitrogen (GO-POPCORN). *Scientific Data*, *9*(1), 688.

Tanioka, T., & Matsumoto, K. (2017). Buffering of ocean export production by flexible elemental stoichiometry of particulate organic matter. *Global Biogeochemical Cycles*,

31(10), 1528–1542.

Teng, Y.-C., Primeau, F. W., Moore, J. K., Lomas, M. W., & Martiny, A. C. (2014). Global-scale variations of the ratios of carbon to phosphorus in exported marine organic matter. *Nature Geoscience*, *7*(12), 895.

Toseland, A., Daines, S. J., Clark, J. R., Kirkham, A., Strauss, J., Uhlig, C., ... others (2013). The impact of temperature on marine phytoplankton resource allocation and metabolism. *Nature Climate Change*, *3*(11), 979.

Tyrrell, T. (1999). The relative influences of nitrogen and phosphorus on oceanic primary production. *Nature*, *400*(6744), 525–531.

Van Den Broeck, N., Moutin, T., Rodier, M., & Le Bouteiller, A. (2004). Seasonal variations of phosphate availability in the SW Pacific Ocean near New Caledonia. *Marine Ecology Progress Series*, *268*, 1–12.

Van Mooy, B. A., Rocap, G., Fredricks, H. F., Evans, C. T., & Devol, A. H. (2006). Sulfolipids dramatically decrease phosphorus demand by picocyanobacteria in oligotrophic marine environments. *Proceedings of the National Academy of Sciences*, *103*(23), 8607–8612.

Van Wambeke, F., Christaki, U., Giannakourou, A., Moutin, T., & Souvemerzoglou, K. (2002). Longitudinal and vertical trends of bacterial limitation by phosphorus and carbon in the Mediterranean Sea. *Microbial Ecology*, 119–133.

von Liebig, J. (1840). *Die organische Chemie in ihrer Anwendung auf Agricultur und Physiologie.* Vieweg.

Wang, W.-L., Moore, J. K., Martiny, A. C., & Primeau, F. W. (2019). Convergent estimates of marine nitrogen fixation. *Nature*, *566*(7743), 205–211.

:

Yoshimura, T., Ogawa, H., Imai, K., Aramaki, T., Nojiri, Y., Nishioka, J., & Tsuda, A. (2009). Dynamics and elemental stoichiometry of carbon, nitrogen, and phosphorus in particulate and dissolved organic pools during a phytoplankton bloom induced by in situ iron enrichment in the western subarctic Pacific (SEEDS-II). *Deep Sea Research Part II: Topical Studies in Oceanography*, *56*(26), 2863–2874.

Yvon-Durocher, G., Dossena, M., Trimmer, M., Woodward, G., & Allen, A. P. (2015). Temperature and the biogeography of algal stoichiometry. *Global Ecology and Biogeography*, *24*(5), 562–570.

Zhao, M., Golaz, J.-C., Held, I., Guo, H., Balaji, V., Benson, R., . . . others (2018). The GFDL global atmosphere and land model AM4. 0/LM4. 0: 2. Model description, sensitivity studies, and tuning strategies. *Journal of Advances in Modeling Earth Systems*, *10*(3), 735–769.
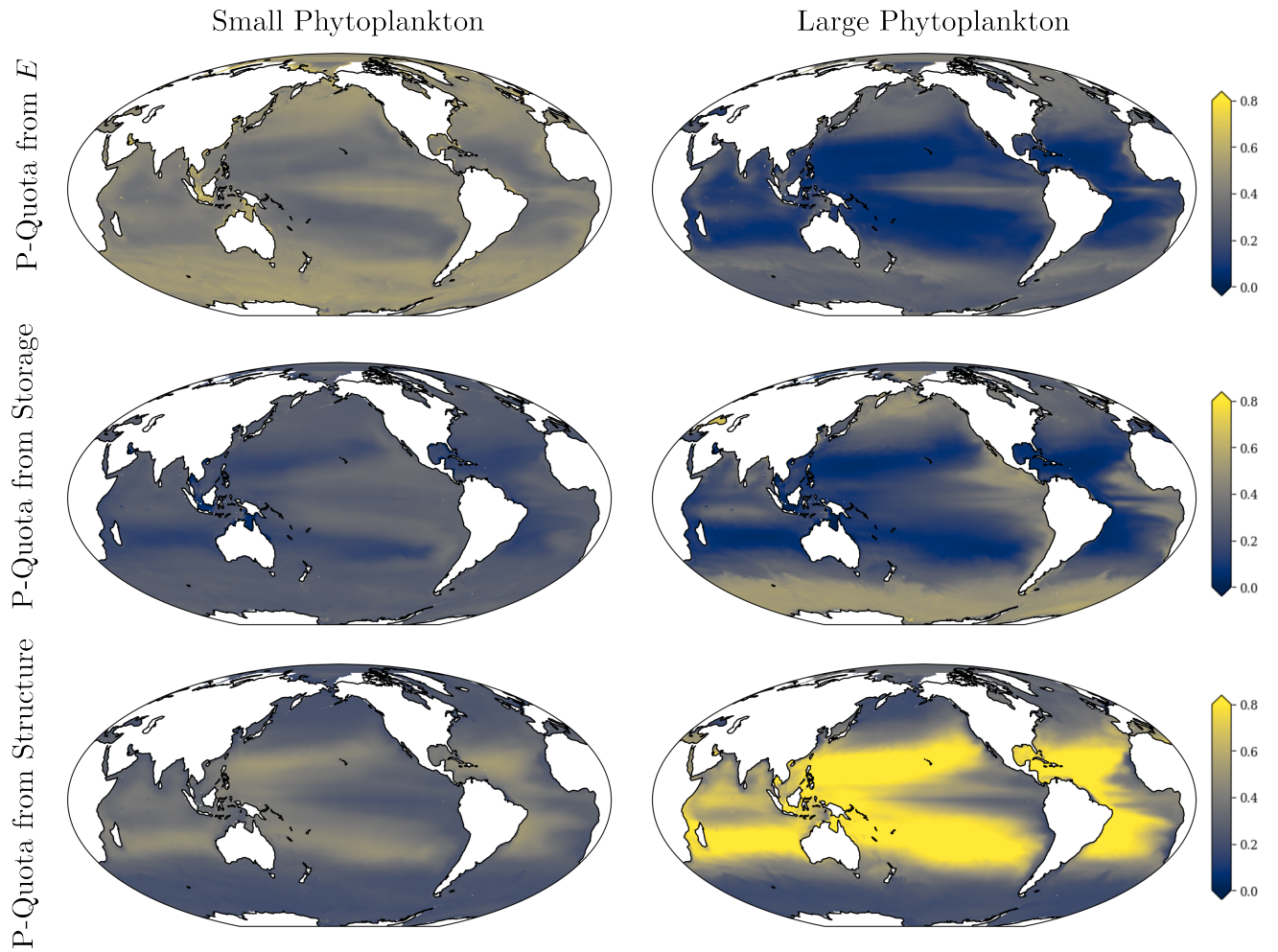
Figure S1. Biomass and productivity weighted average of the contribution of biosynthesis investments, luxury phosphorus storage, and structure to phosphorus quotas in small and large phytoplankton.
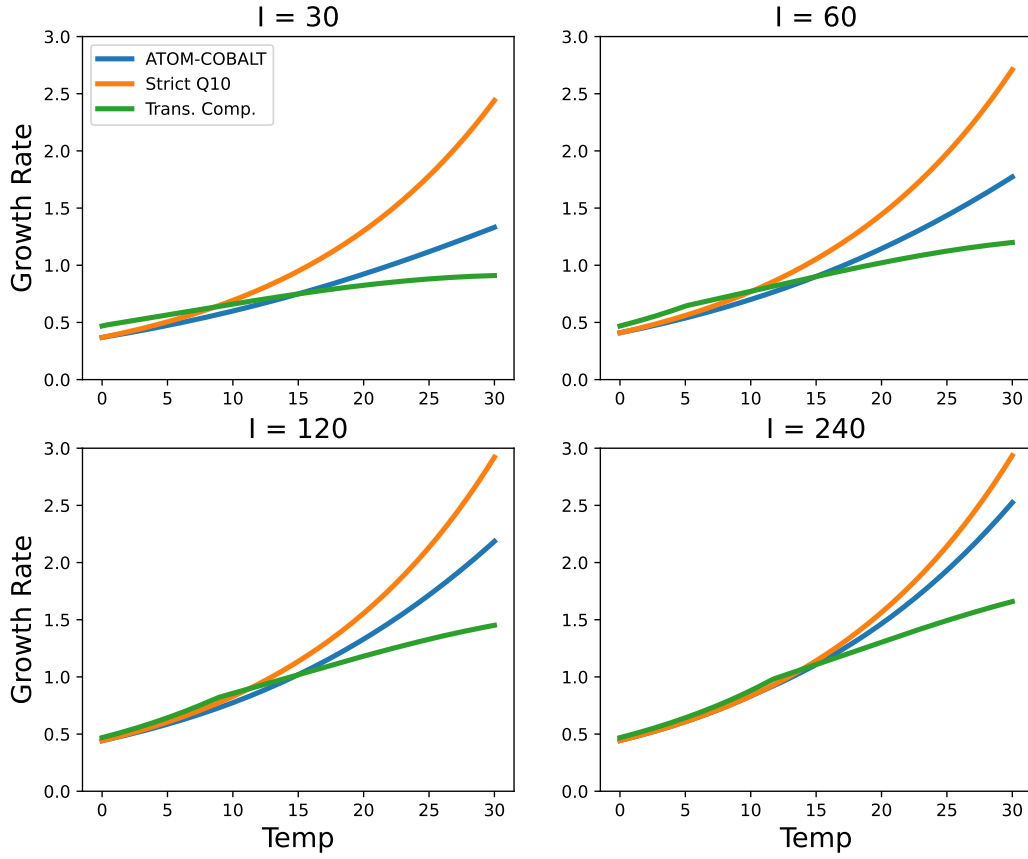
Figure S2.   Temperature scaling of growth rates at different values of irradiance for the ATOM-COBALT and dynamic with translation compensation model. Nutrient concentrations were $[NO_3] = 0.1\mu mol/L$, $[NH_4] = 0.01\mu mol/L$, $[PO_4] = 0.01\mu mol/L$, and an internal Fe quota of $q_{fe} = 1.0$. The strict Q_{10} curve shows the growth rate scaling at κ_{eppley}.
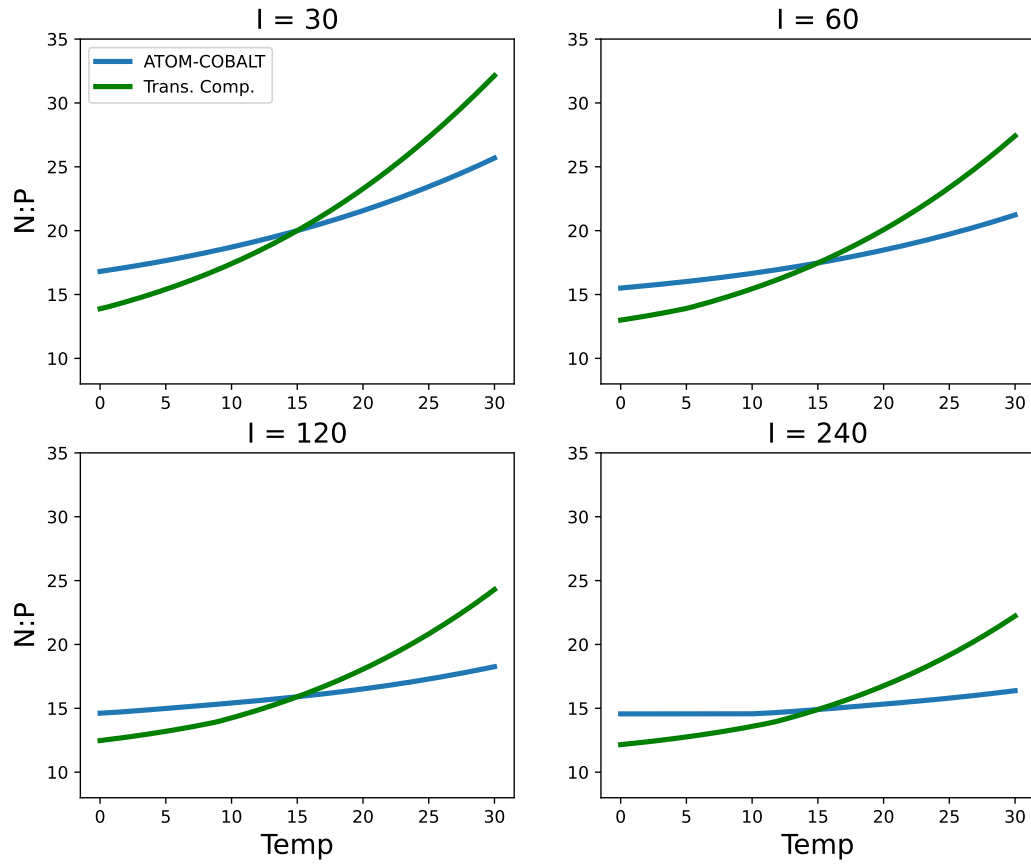
Figure S3. Optimal N:P ratios of small phytoplankton in the ATOM-COBALT model and the dynamic with translation-compensation model. The environmental conditions are identical to Fig. S2.
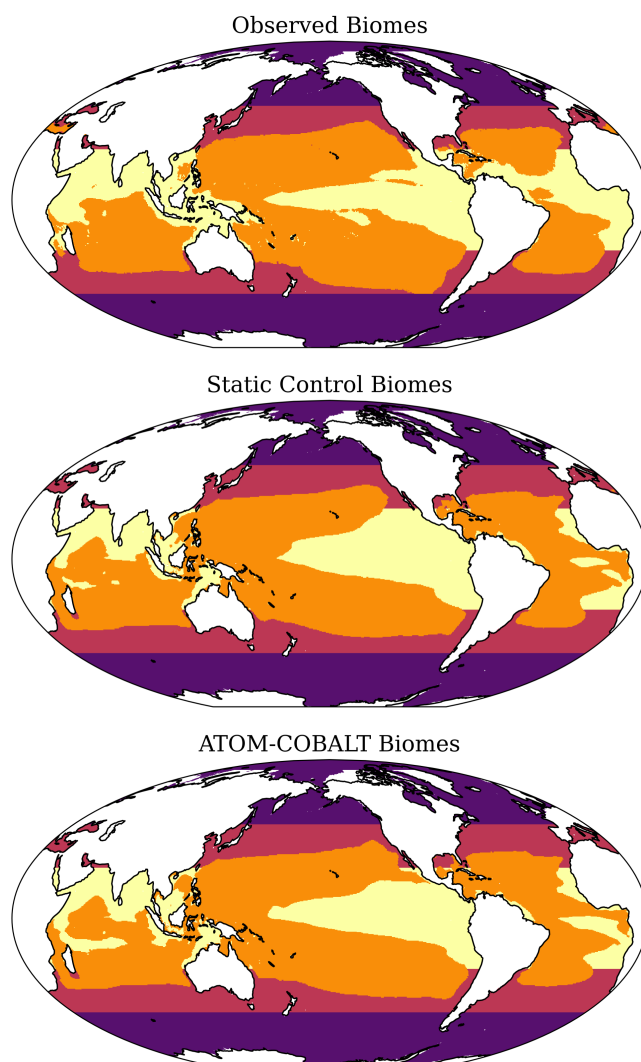
Figure S4. Definition of biomes used for comparison between simulation models and observations.
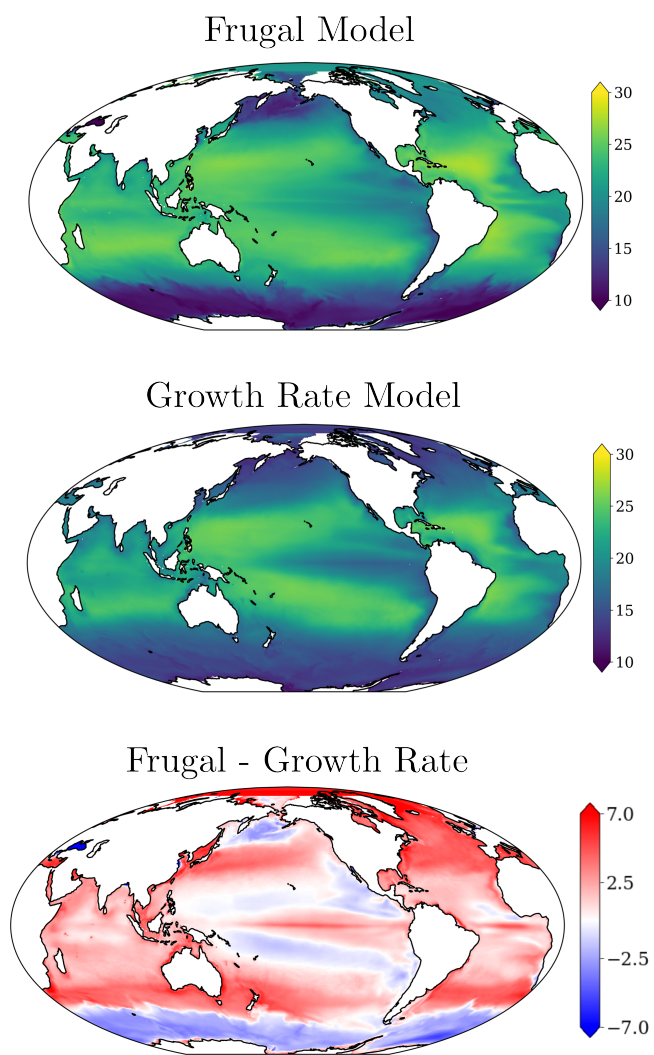
Figure S5. Comparison of export N:P ratios in the frugal and growth rate models.

Cruise	Year	Samples	Latitude	Longitude	Reference
GO-SHIP NH1418	2014	15	-3 to 19	-158 to -150	(Lomas & Martiny, 2020c; C. A. Garcia et al., 2020; Lomas et al., 2021)
GO-SHIP I9N	2016	34	-31 to 18	85 to 110	(Martiny & Lomas, 2021; C. A. Garcia et al., 2018, 2020; N. S. Garcia et al., 2022)
GO-SHIP I7N	2018	38	-30 to 18	40 to 69	(Martiny, Garcia, et al., 2022)
GO-SHIP P18	2016-2017	57	-70 to 29	-116 to -100	(Moreno et al., 2020; Martiny et al., 2020; Lee et al., 2021)
GO-SHIP AMT28	2018	33	-48 to 50	-53 to -6	(Moreno et al., 2022; Larkin et al., 2020; N. S. Garcia et al., 2022)
GO-SHIP $C13\_5$	2020	27	-41 to 35	-74 to 17	(Martiny, Garcia, et al., 2022)
AE1319	2013	16	32 to 55	-69 to -40	(Lomas & Martiny, 2020a; C. A. Garcia et al., 2020; Baer et al., 2017)
SKQ2018-13S	2018	13	63 to 69	-173 to -165	(Tanioka, Larkin, et al., 2022)
SKQ1709s	2019	14	63 to 69	-172 to -164	(Tanioka, Larkin, et al., 2022)
OS1701	2017	29	67 to 72	-169 to -154	(Tanioka, Larkin, et al., 2022)
OS1901	2019	34	63 to 73	-171 to -154	(Tanioka, Larkin, et al., 2022)
SEED	2001	6	49 to 49	164 to 165	(Yoshimura et al., 2009)
X0804	2008	20	20 to 32	-66 to -45	(Martiny, Pham, et al., 2013)
BV39	2007	10	20 to 34	-66 to -64	(Martiny, Pham, et al., 2013)
BV46	2011	15	20 to 39	-66 to -64	(Lomas & Martiny, 2020b; C. A. Garcia et al., 2020; Baer et al., 2017)
X0705	2007	23	27 to 38	-66 to -56	(Martiny, Pham, et al., 2013)
ATP3	2006	13	21 to 32	-66 to -64	(Martiny, Pham, et al., 2013)
BATS	2003 to 2010	61	31 to 32	-66 to -64	(Lomas et al., 2010)
HOT	1989 to 2009	186	23	-158	(Karl et al., 2001)
Atlantic	1973	4	-31	10	(Copin-Montegut & Copin-Montegut, 1983)
MD03/ICHTYO	1974	123	-56 to -24	26 to 78	(Copin-Montegut & Copin-Montegut, 1978)
Tuamotu	1985 to 1996	13	-18 to -15	-148 to -141	(Charpy et al., 1997)
Copin-Montegut	1974	10	-56 to -26	61 to 75	(Copin-Montegut & Copin-Montegut, 1978)
Loh-Bauer	1996	4	-54 to 36	-176 to -122	(Loh & Bauer, 2000)
FluPAC	1994	36	-14 to 6	-179 to -149	(Rodier & Le Borgne, 1997)
BIOSOPE	2004	20	-35 to 8	-141 to -73	(Moutin et al., 2008)
PROSOPE	1999	22	31 to 43	-10 to 22	(Van Wambeke et al., 2002)
DIAPAZON	2002 to 2003	28	-24 to -20	166 to 168	(Van Den Broeck et al., 2004)
Bering Sea	2009 to 2010	27	54 to 63	-179 to -161	(Martiny, Pham, et al., 2013)
BULA/CMORE	2007	7	-16 to 17	-170 to -159	(Hewson et al., 2009)
Medar	1991 to 2001	12	41 to 45	5 to 14	(Fichaut et al., 2003)
NABE	1989	20	18 to 34	-31 to -21	(Passow & Peinert, 1993)
Latitud-II	1995	10	-33 to 25	-45 to -18	(Gasol et al., 2009)
Kahler	2002	10	18 to 32	-20	(Dietze et al., 2004)
OMEX	1993 to 1995	40	47 to 50	-16 to -7	(Bode et al., 2004)
SUPER-HI-CAT	2008	13	28 to 35	-155 to -138	(Clemente et al., 2010)

Table S1. Sources of data on N:P ratios of particulate organic matter